Influence of Foaming Process on Acoustic Performance of a Vehicle with a Typical Lightweight Floor Carpet

Yi Huang[1(✉)], Yuqing Ge[1(✉)], Weiqiang Liang[2(✉)], Lin Liu[1], and Ding Li[1]

[1] CAE Center, Changan Automotive Engineering Institute, Chongqing, China
hy-sy2000@163.com, yuqing_ge@126.com
[2] NVH Center, Changan Automotive Engineering Institute, Chongqing, China
278116054@qq.com

Abstract. This article focuses on the effect of different foaming process on acoustic performance of a vehicle with a typical vehicle lightweight floor carpet. The carpet structure difference between 2 different foaming processes was discussed firstly. A statistical energy analysis (SEA) based transmission loss model was developed to predict the sound transmission loss (STL) under different boundary conditions. It was found that the STL of the carpet with direct foaming process is much worse than the separate foaming process carpet when the boundary condition was Bonded-Bonded. Then a full vehicle SEA model was developed to predict the sound pressure level (SPL) at the front-left (FL) driver's headspace. In parallel, a test was conducted to measure the SPL response at the same space after the floor was assembled on the vehicle. The test results showed the good agreement with the simulation results.

Keywords: Floor carpet · Lightweight · Foaming process · Acoustic · Simulation · SEA · STL

1 Introduction

The floor carpet of the vehicle is a very important sound package part for high frequency acoustic performance on road noise and engine/motor noise. Lightweight is the vehicle design tendency due to the demand of vehicle fuel economy. More and more vehicle floor carpets are made of absorption layers instead of mass layer. Carpet substrate made with high-density felt plus Polyurethane (PU) foam is a typical lightweight structure.

NVH sound package researchers have studied on the acoustic performance of many different structure of floor carpets including lightweight carpet [1–3, 10]. Also, a lot of work has been taken on the research of double-wall structure to study the transmission loss performance [4–7]. However, nobody concerned about the manufacturing process influence on the acoustic performance. In this article, we mainly studied the foaming process influence on the acoustic performance for the typical felt plus PU floor carpet. We found that the structures and the acoustic performance will be different if the foaming process was different for this carpet.

China Society of Automotive Engineers: *Proceedings of China SAE Congress 2021: Selected Papers*, LNEE 818, pp. 1004–1016, 2023.
https://doi.org/10.1007/978-981-19-3842-9_78

2 PU Foaming Process and Carpet Structure

The raw material for PU is called as Material-A and Material-B. PU material will be foaming once the Material-A is mixed with Material-B. High pressure will be produced when the PU material is foaming. There are 2 different foaming process for vehicle carpet. One is direct foaming and the other is separate foaming as shown in Fig. 1(a) and 1(b) separately.

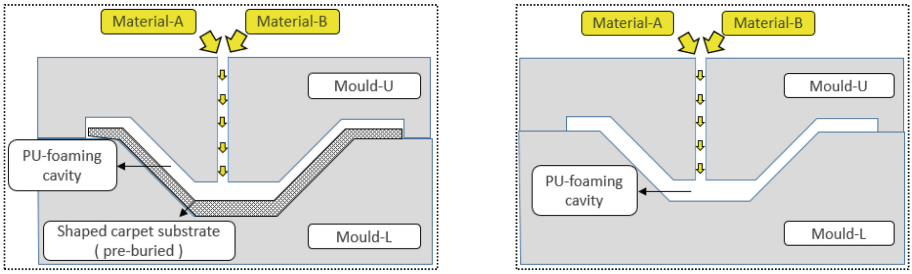

(a). Direct foaming process (b). Separate foaming process

Fig. 1. Two different foaming processes

Currently the structure design of the typical lightweight carpet is: PET needle punched fabric (500 g/m^2) + High density felt (600 g/m^2) + PU foam (55 kg/m^3) as shown in Fig. 2.

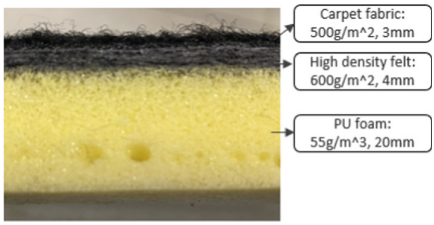

Fig. 2. A typical lightweight vehicle carpet

If the separate foaming process is used, foamed PU layer will be glued onto the felt layer. The carpet structure will be same as the design as shown in Fig. 3(a). If the direct foaming process is used, PU material will penetrate into the adjacent felt layer and fill the porous holes under the high pressure during the forming process. Then the felt layer will almost lose its absorption capability and become a septum mass layer as shown in Fig. 3(b), which differs from the original design structure.

However, the manufacturing engineer usually takes the direct foaming as the process due to the lower cost. Since the process has the effect on the carpet structure, it is necessary to see how much influence on NVH performance. This issue has never been concerned by NVH researchers.

Next section will discuss the acoustic performance of these two floor structures.

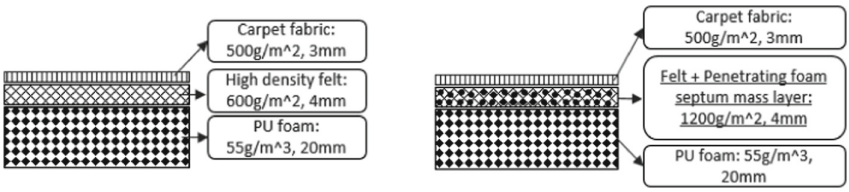

(a) Separate foaming process (b) Direct foaming process

Fig. 3. Carpet structure comparison with different foaming process

3 Simulation Analysis

3.1 Modeling of PU Material and Boundary Conditions

Modeling of PU Material. PU foams, which is widely used in the automotive industry, is an elastic porous material. It is modeled based on the extension of the Biot theory [11, 13]. Different with the other absorption material, PU foam has a micro-structure of honeycomb frame as shown in Fig. 4(a). The in vacuo bulk modulus of this frame is of the same order as that of air, and as a result both the frame and fluid take a significant and distinct role in the wave propagation process. It can support three wave types simultaneously: solid and fluid compressional waves and shear wave as Fig. 4(b) shows. It requires all the fluid properties and the elastic bulk properties, totally 9 parameters as shown in Table 1.

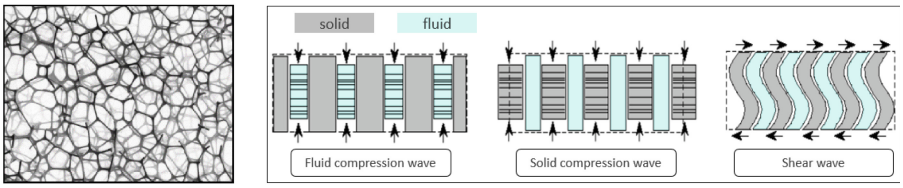

(a) Micro-structure of foam (b) Two compression waves and one shear wave

Fig. 4. PU foam micro-structure and three types of wave

Modeling of Two Types Process of Carpet. The vehicle floor system with seperate PU foaming process carpet was modeled as Fig. 5 shows. At this condition, the upside of the foam layer is normally glued with the felt layer. The downside of the foam layer is probably bonded or unbonded to the floor steel panel depending on the match and assembly. The vehicle floor system with direct PU foaming process carpets was modeled as Fig. 6 shows. At this condition, the upside of the foam layer is tightly contacted with the felt layer due to the PU penetrating during the foaming process. The downside of the foam layer is probably bonded or unbonded to the floor steel panel depending on the match and assembly.

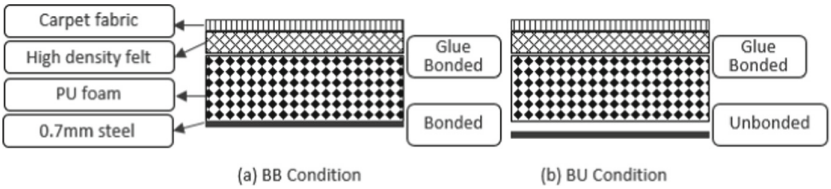

Fig. 5. Separate PU foaming process carpet modeling

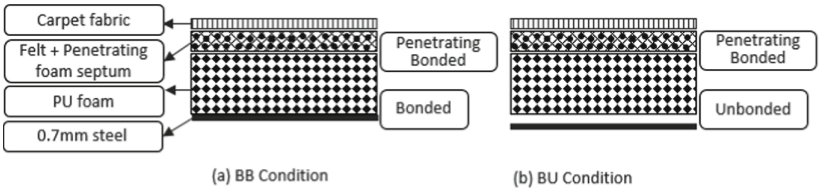

Fig. 6. Direct PU foaming process carpet modeling

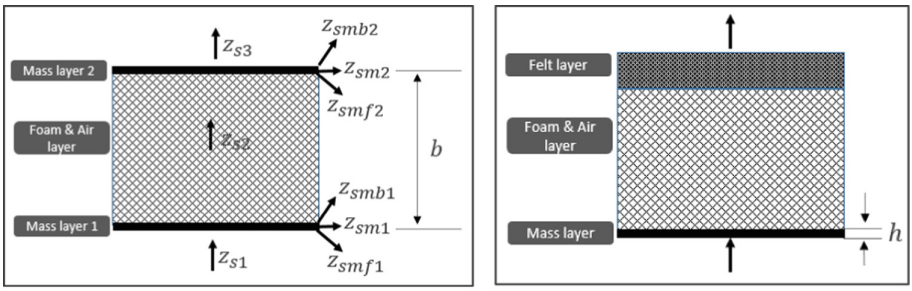

Fig. 7. Two types of BB boundary condition (a). BB condition for direct foaming process dual-mass sound insulation system (b). BB condition for separate foaming process single-mass sound insulation system

Boundary Condition. When the direct foaming process is used, the carpet together with the floor panel will be a dual-mass system. The impedance of each layer for BB condition of this system is shown in Fig. 7(a).

In this case, since the panel is directly attached to the solid phase of the porous material, the normal velocities of the solid and fluid phases are constrained to be equal to each other. As a result of the velocity constraint, the impedances of the air-borne and structure-borne waves add in series. In this case response is controlled by the structure-borne impedances, and compression and shear waves in the frame may be the most important [4, 8].

In terms of the equivalent impedance method [14], the STL equation for dual thin mass panel is given by:

$$\mathrm{R} = 10\log\left|\frac{1}{t_p^2}\right| = 10\log\left|\frac{\left(Z_{sm1f}+Z_{s1}\right)^2}{4Z_{sm1f}Z_{s1}}\right| \tag{1}$$

$$Z_{sm1f} = Z_{sm1} + Z_{sm1b} \tag{2}$$

In terms of the impedance transfer equation [14], the equivalent impedance of the back surface of mass layer 1 is:

$$Z_{sm1b} = Z_{s2}\frac{Z_{sm2f}\cos(kb) + jZ_{S2}\sin(kb)}{Z_{s2}\cos(kb) + jZ_{sm2f}\sin(kb)} \tag{3}$$

$$Z_{sm2f} = Z_{sm2} + Z_{sm2b} \tag{4}$$

$$Z_{sm2b} = Z_{s3},\ Z_{sm1} = jm_1\omega,\ Z_{sm2} = jm_2\omega,\ Z_{s1} = Z_{s3} = \rho_0 c_0 \tag{5}$$

where: R is the STL of the system, t_p is the transmitted coefcient, k is the wave number, b is the gap between the 2 mass layer, m_1, m_2 is the surface density of mass layer 1 and 2, ω is the circular frequency, $\rho_0 c_0$ is the characteristic impedance of air, Z_{s1} is the medium impedance of incident wave, Z_{sm1f} is the front surface impedance of mass layer 1, Z_{sm1}. is the impedance of the mass layer 1, Z_{sm1b} is the back surface impedance of mass layer 1, Z_{s2} is the impedance of the medium between the 2 mass layers, Z_{sm2f} is the front surface impedance of mass layer 2, Z_{sm2} is the impedance of the mass layer 2, Z_{sm2b} is the back surface impce of mass layer 2, Z_{s3} is the medium impedance of transmitted wave.

$$Z_{s2} = \frac{K_b}{j\omega} \tag{6}$$

$$K_b = \frac{E(1+j\eta)}{3(1-2\vartheta)} \tag{7}$$

where: Z_{s2} is the impedance of the foam layer as a spring structure. K_b is the bulk modulus of the foam frame, E is the Young's Modulus of the foam, η is the damping loss factor of the frame, ϑ is the Poisson's Ratio of the foam. The k in Eq. (3) will be the wave number in the foam structure, which is different with that in the air and detailed discribed in the reference [13].

Combined the Eq. (1) to (7), the solution of R can be solved. The expression of R was so complicated that we need turn to the software VA One for help. The modeling of STL will be decribed in the next section. The resonance frequency for the case represented in this paper was about 1250 Hz, which is higher than the resonance frequency of mass-air-mass system, about 500 Hz. The STL dip can be found in Fig. 9(a). The STL can also be caculated with direct global matrix (DGM) method for this kind of structure in reference [4, 9] written by Brian H. Tracey and J.S. Bolton.

When the seperate foaming process is used, the carpet together with the floor panel will be a mass-absorption system as shown in Fig. 7(b). There is a coincidence frequency

f_c for a single layer panel given by Eq. (7). In terms of this equation, the resonance frequency f_c for a 0.7 mm steel panel is about 20000 Hz, which is far away from the human sensitive frequency range. In contrary with the dual-mass system, the elastic properties of bonded PU layer contributes to stiffen the BB structure and reduce the coincidence frequency. Dual to the increased bending rigidity B, the coincidence frequency meets around 2500 Hz for this case. The STL dip can be found in Fig. 9(a).

$$f_c = \frac{c^2}{2\pi}\sqrt{\frac{m}{B}} \tag{8}$$

where m and B is the surface density and bending rigidity of the mass layer seperately.

On the other hand, when the elastic porous material is not bonded directly to an elastic panel. In this case, the relatively well damped airborne wave is the major energy carrier. The acoustic performance is different with the bonded condition.

The acoustical performance of a foam layer may appear to be completely different depending on whether it is directly attached to a facing panel, or whether it is separated from it by a small air gap. Thus, when using elastic porous materials in noise control treatment it is very important to understand the effect of boundary conditions on the installed performance of a treatment so that the optimum arrangement can be chosen in each particular instance.

The STL performance result of this typical lightweight floor carpet with different boundary condtions and different manufacturing process will be discussed in the next section.

3.2 STL Simulation

The Software VA One was used to simulate the acoustic performance of the main floor. A STL model including a reverberation source cavity, a 1 m * 1 m * 0.7 mm flat steel panel and a receiving cavity shown in Fig. 8 is established in VA One. The main floor is configured as a multi-layered material and applied to the STL mode [12, 13]. The effective transmission loss is calculated using the following Eq. (8):

$$\mathrm{TL} = 10\log_{10}\left(\frac{A\omega}{8\pi^2 c_1^2 n_1 \eta_2}\left(\frac{E_1}{E_2} - \frac{n_1}{n_2}\right)\right) \tag{9}$$

where

A is the effective transmission area of the junction;
c is the acoustic wave speed in the source cavity;
ω is the center frequency of the band (in rad/s);
η is the damping loss factor of the receiving cavity;
E is the cavity subsystem energy;
n is the cavity subsystem modal density (in modes/(rad/s)).
The subscripts 1 and 2 refer to the source cavity and receiving cavity respectively.

The Tables 1, 2 and 3 lists the material properties of noise control layers used in the main floor structure.

Considering that the PU foam is very sensitive to the boundary condition, both **Bonded-Bonded (BB)** and **Bonded-Unbounded (BU)** conditions were studied for this

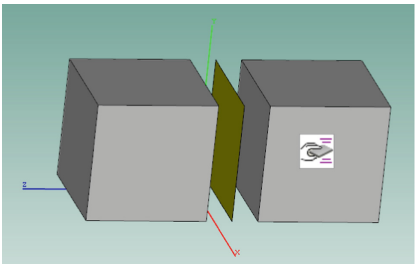

Fig. 8. STL model for flat floor carpet sample

Table 1. The property of PU foam

PU foam (name: foam_55 kg/m^3)			
Density (kg/m^3)	55	Thermal c.l. (m)	0.00016
Flow resistivity (N.s/m^4)	42000	Damping loss factor	0.2 (elastic parameter)
Porosity	0.95	Young's Modulus (Pa)	9e5 (elastic parameter)
Tortuosity	2.4	Poisson's ratio	0.3 (elastic parameter)
Viscous c.l. (m)	8e−5		

Table 2. The property of recycle cotton felt

Cotton felt (name: felt_150 kg/m^3)			
Density (kg/m^3)	150	Tortuosity	1.8
Flow resistivity (N.s/m^4)	75000	Viscous c.l. (m)	5.6e−5
Porosity	0.9	Thermal c.l. (m)	0.0002

Table 3. The property of needle punched fabric felt

Floor needle punched fabric felt (name: carpet_needled_fabric_500g/m^2)			
Density (kg/m^3)	125	Tortuosity	1.05
Flow resistivity (N.s/m^4)	9000	Viscous c.l. (m)	0.00002
Porosity	0.95	Thermal c.l. (m)	0.0002

lightweight floor carpet as shown in Fig. 6. The PU layer is glued or penetrated to the felt layer so the upside condition of PU layer is always Bonded. The downside condition is Bonded or Unbounded depending on whether the PU layer attaches to the floor panel or not.

The following tables give the modeling details of two different floor layers in VA One, direct foaming process floor carpet as Table 4 and separate foaming process floor carpet (design intention) as Table 5.

Table 4. Layers of the direct foaming PU floor carpet (BB & BU)

Layer	Type	Solid material	Fluid material	Thickness [m]	Loss factor	Remark
Structure side						
1	Gap	None	Air	0.001	0	For BU
2	Foam	PU_55 kg/m^3	Air	0.02	0.2	/
3	Septum	None		0.004	0	/
4	Fiber	fabric_500 g/m^2	Air	0.002	0	/
Fluid side						

Table 5. Layers of the separated foaming PU floor carpet (BB & BU)

Layer	Type	Solid material	Fluid material	Thickness [m]	Loss factor	Remark
Structure side						
1	Gap	None	Air	0.001	0	For BU
2	Foam	PU_55 kg/m^3	Air	0.02	0.2	/
3	Felt	Felt_150 kg/m^3	Air	0.004	0	/
4	Septum	None		0.0003	0	/
5	Fiber	fabric_500 g/m^2	Air	0.002	0	/
Fluid side						

Figure 9 (a) shows the simulating results of STL of 2 different process carpets (PU thickness: 20 mm) respectively under BB and BU boundary conditions. For direct foaming process carpet, the STL is about the best one under BU boundary condition but the worst one under BB boundary condition. For separate foaming process carpet, its STL performance is between the direct foaming process carpets under BU&BB boundary conditions. Compared with BU boundary condition, the STL performance of BB boundary condition drops 5–10 dB at above 1250 Hz. The simulating result shows that BB boundary condition degrades the STL performance compared with BU. Especially for direct foaming process carpet, it degrades most. The floor carpet is bonded to the floor panel naturally due to the gravity of the earth. The floor carpet will attach to the floor panel more or less no matter which type of floor carpet. Thus, the direct foaming process isn't preferred due to the acoustic performance degradation for floor carpet. The same conclusions can be seen for 10 mm thickness PU in Fig. 9(b). The reason for the STL dip presence was clarified in Sect. 3.2.

The influence on the STL performance for different penetrating percentage was additionally studied. The result showed the familiar phenomenon for 50%, 75% and

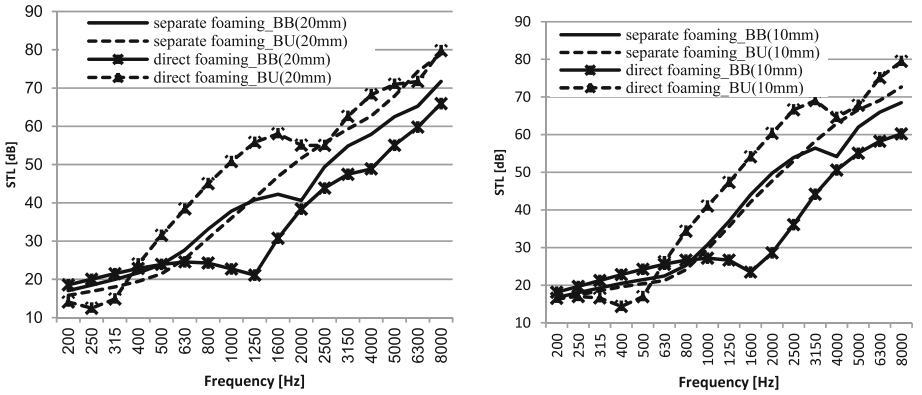

(a) PU thickness: 20mm (b) PU thickness: 10mm

Fig. 9. STL of different process carpets and boundary conditions

100% percentage in Fig. 10. That means the STL degradation is very sensitive to the penetrating of PU foam.

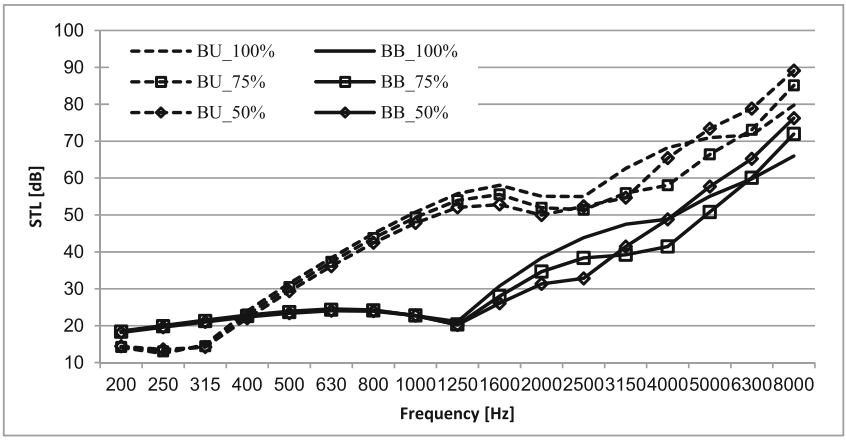

Fig. 10. STL of different penetrating percentage for direct foaming process carpet

The full vehicle acoustic performance of these floor configurations will be discussed in the next section.

3.3 Full-Vehicle Simulation and Test Validation

A full vehicle level Statistic Energy Analysis (SEA) model was established in VA One as Fig. 11 shows. The interested frequency is from 200 Hz to 8000 Hz in 1/3 Octave. A calibration experiment was conducted in parallel to debug the SEA model. A vehicle

with direct foaming process floor carpet was taken for the test. The test was in a semi-anechoic room and was excited by a point source placed at the tire. Three microphones were uniform distributed in the cavity related with the SEA model both inside and outside of the car to measure the sound pressure. Figure 12 shows that the SEA prediction was in good agreement with the experiment results with a variation of less than 3 dB.

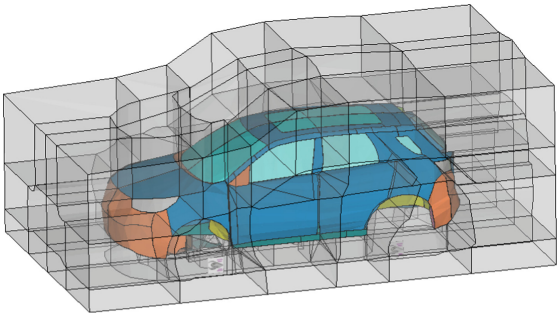

Fig. 11. Full vehicle SEA model

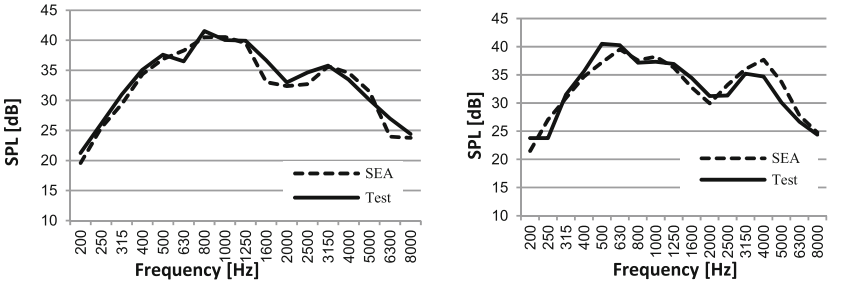

(a) SPL of FL head to FL tire excite (b) SPL of RR Head to RR tire excite

Fig. 12. Simulation vs. test result

By calibrating the SEA model, it was found that both bonded and unbounded boundary conditions for PU floor layers were presented. The carpet in the foot area and the under seats area was bonded and the rest area unbounded.

Both the direct foaming process carpet and the separate foaming process carpet configurations were created in SEA model. The SPL of FL driver's head cavity with the FL tire excited by point sound source is shown as Fig. 14(a). It can be seen that the separated foaming process PU carpet performs 1–3 dB better than the direct foaming process carpet at 400–2000 Hz which is in coincidence with the predictions in 3.1 & 3.2. The SPL at above 3150 Hz did not show any difference because the floor area was not the dominated path in full vehicle.

Both the direct foaming process carpet and the separate foaming process carpet were manufactured for the test as Fig. 13 shows. The tests were conducted in a semi-anechoic chamber. Same as the simulation, the vehicle was excited by a point sound source at FL

tire and the SPL at FL driver's head cavity was measured. The test sequence was firstly with the original direct foaming process carpet, then with the separated foaming process carpet and at last with the original carpet again.

(a) Direct foaming process carpet

(b) Separate foaming process carpet

Fig. 13. The floor carpets manufactured for test

The test result was in line with the simulation as the Fig. 14(a), (b) shows. The separate foaming process carpet performs 1–5 dB better than the original direct foaming carpet at 400–2000 Hz. Note that the original floor carpet reinstalled at last also performs better as Fig. 14(b) shows. Obviously, the reinstallation changed the boundary condition of the PU layer. It can be concluded that the acoustic performance of the vehicle with direct foaming process floor carpet might become worse and worse due to the tighter bonded boundary condition as time goes by.

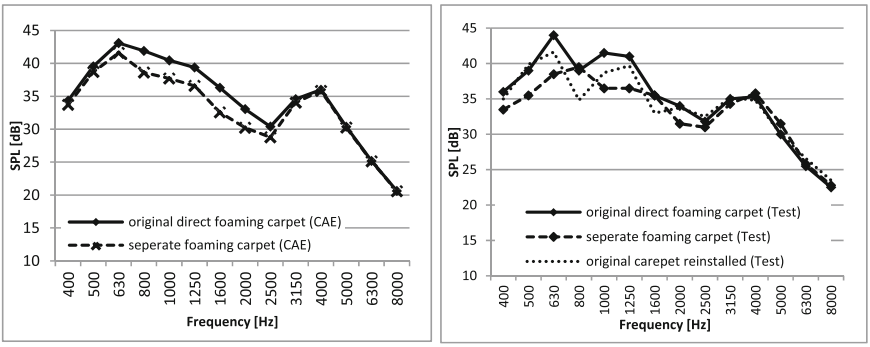

(a) Simulation results

(b) Test results

Fig. 14. SPL at FL Driver's head for simulation and test

The on-road test was also conducted. The details is not included in this paper. The rough conclusion was that the speech articulation index performance with separate foaming process carpet was 6%–9% better than with the direct foaming process one. As a

result, the direct foaming process is NOT recommended for the typical lightweight floor carpet.

4 Conclusions

This paper has presented a new finding and simulation technique for the acoustic performance of the vehicle with typical lightweight foam-type floor carpet under different foaming process. Both material SEA model and full vehicle SEA model showed the bonded condition to floor panel will degrade the acoustic performance. Especially for the direct foaming process carpet, it degraded most. A full vehicle test was conducted in parallel to validate the simulation result. Good agreement between the test data and the simulation was achieved.

It has also been shown that wave propagation in elastic porous materials can be modeled accurately based on the Biot's general elastic porous material theory. It's seen that the acoustic performance degradation at frequency of 400 Hz to 2000 Hz for direct foaming process due to the foam elastic character.

For most of sound package parts, manufacturing process was a very important factor for the acoustic performance of the part besides the structure design. Our results demonstrated not only the STL degradation but also the possibility of the acoustic performance variation with assembly and time history difference for lightweight foam-type carpet. The direct foaming process was NOT recommended for the floor carpet process design of vehicle. The separate foaming process or felt material was preferred to eliminate this degradation.

References

1. John, T.K., Wang, X.: Vehicle floor carpet acoustic optimization using statistical energy analysis. Int. J. Veh. Noise Vib. **5**, 141–157 (2009)
2. Wentzel, R.E.: An interactive approach to the design of an acoustically balanced vehicle sound package. In: SEA (2007)
3. Lupea, I.: Considerations on the vehicle floor carpet vibro-acoustic modeling. Appl. Math. Mech. **56**(2), 263–268 (2013)
4. Bolton, J.S.: Sound transmission theory through multi-panel structures lined with elastic porous materials. J. Sound Vib. **191**(3), 317–347 (1996)
5. Zhou, J.: Optimization for sound transmission through a double-wall panel. Appl. Acoust. **74**, 1422–1428 (2013)
6. Liu, Y.: Effects of external and gap mean flows on sound transmission through a double-wall sandwich panel. J. Sound Vibr. **344**, 399–415 (2015)
7. Wang, J.: Sound transmission through lightweight double-leaf partitions: theoretical modeling. J. Sound Vib. **286**, 817–847 (2005)
8. Bolton, J.S.: Elastic porous materials for sound absorption and transmission control. In: International Congress on Noise Control Engineering (2005)
9. Tracey, B.H.: Transmission loss for vehicle sound packages with foam layers. In: Noise and Vibration Conference and Exposition (1999)
10. Lee, H.R.: Application of global sensitivity analysis to statistical energy analysis: vehicle model development and transmission path contribution. Appl. Acoust. **146**, 368–389 (2019)

11. Allard, J.F.: Propagation of Sound in Porous Media. Elsevier, Amsterdam (1993)
12. VA One 2014 User's Guide
13. VA One 2014 Foam Module User's Guide, Theory & QA
14. 何琳, 声学理论与工程应用 (2006)